PHYSICAL REVIEW B VOLUME 19, NUMBER 12 15 JUNE 1979

Halogen charge-transfer excitations in alkali metals

R. Avci and C. P. Flynn
Department of Physics and Materials Research Laboratory, University of Illinois at Urbana-Champaign, Urbana, Illinois 61801
(Received 18 January 1979)

The excitation spectra of halogen impurities in alkali metals have been investigated by vacuum-uv spectroscopic methods. We observe threshold energies for the charge-transfer excitation that agree quantitatively with the earlier predictions by Flynn. The deduced Stokes shifts are almost independent of impurity species and compatible with the observed threshold broadening. Continuum absorption observed below threshold is probably due in part to impurity-induced electron scattering. There is a clear indication that the charge-transfer excitation couples to these continuum processes and produces a Fano-like interference in the optical density. Although the absorption profiles above threshold bear a marked resemblance to those of the analogous salts, most of the structure at higher energy remain poorly understood. The profile near threshold in the metal is identified as a specific *chemical* property of the impurity species. However, the form of the profile cannot be predicted reliably using current theories.

I. INTRODUCTION

The research reported in this paper bears a close relationship to that in the preceding paper[1] (referred to as I in what follows). There we describe the ionic configurations adopted by impurities in alkali metals. Literature references in this area are collected in Paper I. For the present purposes the significant result is that halogen impurities in alkali-metal host lattices exist in well-defined ionic configurations as singly charged negative ions. The lattice remains locally neutral because the electron gas is repelled from the impurity; the screening hole thus formed in the conduction-electron distribution neutralizes the ionic charge. A consequence of screening is that the overlap between band states and the full p^6 outer shell of the halogen ion is greatly reduced. For the main part, the ion experiences only a Madelung-like potential well due to the combined effects of the alkali lattice and the electron gas. The theory of these impurity centers has been developed by Flynn and Lipari.[2]

In the present paper we investigate the electronic excitation spectra of halogen impurities. The important effects are connected with optically induced charge transfer from the negative ions to the host electron gas. Halogen ions have no bound excited states of the outer shell in vacuum. It has been shown by Flynn[3] that in the metal, also, an electron excited from the halogen $(p^6)^-$ outer shell becomes part of the electron gas. The neutral halogen atom left behind still repels the electron gas to locally neutralize the lattice. For this reason the overlap of the excited configuration with the electron gas also remains weak. This led to a suggestion that the excited configuration is sufficiently long lived that it may appear as a sharp feature in the optical excitation spectrum of the alloy.[3] These processes are termed *charge-transfer excitations* because their principal effect is to transfer an electron from the ion to the alkali host lattice. The conduction-electron densities of the two basic configurations are sketched in Fig. 1.

Detailed predictions of the total energy difference between the ground and excited configurations have been given for a variety of halogen-alkali systems. For a description of these calculations the reader is directed to Ref. 3. In what follows we report the observation of the predicted charge-transfer excitations for a number of halogens and alkali metals. The data confirm the predictions and reveal in addition some unexpected and interesting effects.

Local excitations of this type in metals produce persistent spectra that have received much recent attention through their relevance to the behavior

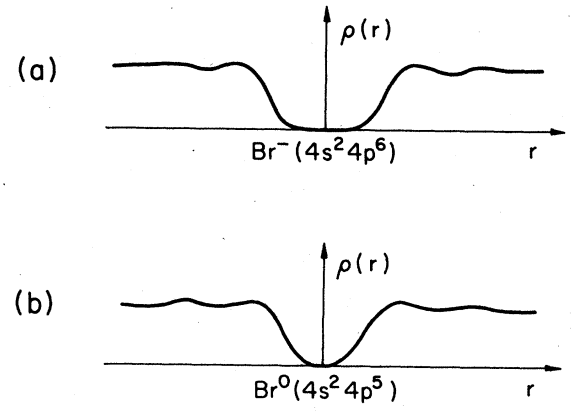

FIG. 1. Conduction-electron densities $\rho(r)$ for ground (a) and excited (b) configurations of halogen impurity in metal.

of a locally shocked electron liquid. The basic impurity excitation spectrum takes a form that reproduces itself to some degree independently of the host lattice in which the active center is embedded (persistence). It does so because the excitation spectrum is most strongly influenced by local configurations of the active center itself; the host structure is less relevant in both the ground and the excited configuration. These persistent profiles are of considerable interest for the information they contain about the locally excited structures. Theoretical predictions in this area are, however, very difficult to obtain accurately, so that quantitatively successful theories of either host or impurity persistent profiles are largely lacking. An exception exists in the case of rare gas-alkali metal alloys for which one-electron spectra have been predicted by Kittler and Falicov.[4] In contrast to this general difficulty with the absorption profile is the fact that the excitation *thresholds* themselves can be calculated accurately by methods developed for impurities, as pointed out by Flynn and Lipari,[5] and confirmed by several later workers.[6,7] The charge-transfer thresholds observed in the present work also conform well to theoretical predictions.

Persistent excitation spectra in metals are of particular interest for the complication caused by the presence of conduction electrons. In one-electron theory, all the band orbital of a metal are deformed by the change of local potential that accompanies a local excitation. Electron-hole pairs are formed in the recoil process that takes place when band orbitals of the ground state project into the distorted orbitals. This added energy absorption produces a high energy tail above each threshold in the excitation spectrum. Its form is predicted by a theory due to Mahan[8] and to Nozières and De Dominicis.[9]

In its application to host core excitations the theory has been the source of considerable controversy. The threshold behavior was initially thought to conform the theory. However, some of the effects have later been interpreted as originating in a variety of other causes, including phonon broadening[10] and the energy variation of band-structure matrix elements.[11] Recent calculations[12] have indicated that, even in the independent particle model, the theoretical profile may be valid in an energy range extending only a small fraction of the Fermi energy above threshold. In the single investigation of impurity spectra that has been reported, the theory gives quite incorrect predictions for the threshold behavior.[13] These earlier investigations concerned rare-gas impurities in alkali-metal hosts, for which the ground and excited configurations are rather well understood. Calculations by Kittler and Falicov[4] have shown that the spectrum above threshold can be predicted quite well by methods that neglect recoil effects entirely. It will emerge in the present paper that halogen impurities in alkali metals also possess predictable ground- and excited-state energies. Consequently, they offer a new opportunity to compare predicted threshold profiles with those observed experimentally.

Some experimental matters will be mentioned briefly in Sec. II, and the observed spectra presented in Sec. III. Section IV contains a discussion of several interesting phenomena that the data reveal.

II. EXPERIMENTAL DETAILS

No new techniques were required to prepare samples or make the optical measurements. The optical equipment used in this work was identical with that described by Phelps *et al.*[13] In brief, it employs a Hanovia H_2 lamp and a normal-incidence grating monochromator to provide two light beams passing through two samples and choppers to a detector. Following phase-sensitive detection, the system output is processed to give the logarithm of the ratio of the two transmitted beams. To use these capabilities to best advantage the two samples were prepared simultaneously with equal quantities of host metal from a single evaporation stream which impinged onto a LiF window held at liquid-He temperature. One of the two samples was also exposed at the same time to a beam of impurity, thereby fabricating the alloy. Under these circumstances, the equipment output was exactly the change in transmission caused by the impurity alone. These are the impurity absorption spectra presented in Sec. III.

A small departure from this precise procedure was made in much of the work reported here. Halogen gases are corrosive and difficult to handle. They are also diatomic. Direct doping with halogen gases could possibly produce pairs of neighboring halogens in the metal host lattice. Short-range order of this type would not be desirable in the present investigations. For these reasons, most of the alloys were prepared by simultaneous evaporation of the metal and the appropriate salt (e.g., K and KBr to produce Br in K). The vapor of this salt consists overwhelmingly of K^+Br^- molecules, so the dilute alloys produced in this way are quite random. Both the reactivity and the short-range-order problems are thus avoided.

In point of fact, auxiliary experiments mentioned

in Sec. III show that samples prepared using the diatomic halogen gas have spectra that are almost identical with those of alloys fabricated by evaporation of the alkali halide. It is very likely that the halogen molecules dissociate as negative ions on contact with the metal, and that the short-range order then becomes essentially random. The important point for the present purposes is that the use of halide evaporations avoided all short-range order, but that the spectra so obtained are for halogen impurities *together with one added host atom*.

The data presented in Sec. III were all obtained for samples fabricated on substrates maintained near 5.5 K in a belljar vacuum of $\sim 3\times10^{-7}$ Torr. It is presumed that the effective vacuum was much lower inside the He can; no sample deterioration could be observed over the course of many hours. The host and impurity evaporation streams were monitored by means of quartz crystals, as described elsewhere.[13,14] In this way, the sample compositions were determined with sufficiently high accuracy that the uncertainty is of no concern in the work described here. Absolute determinations of the film thickness relied on theoretical calibration constants of the crystals,[14] and could be in error by 10%. Direct measurements of film profiles indicated that the calibrations were at least this accurate. The available precision in thickness is of considerable value because it allows the collection of *absolute* absorption intensities.

III. RESULTS

The 20 systems formed by five alkalies and four halogens proved too numerous for exhaustive study in the present investigation. After some survey work it was decided to focus the main effort on certain chosen components. For a variety of reasons, potassium turned out to be an optimum host lattice, bromine an impurity providing excellent, detailed spectra, and fluorine the impurity with the most unexpected behavior. A considerable fraction of the data, therefore, involve one or more of these particular elements.

A. Concentration dependences

Figures 2–5 show spectra observed with various concentrations of Br in Cs, Br in Rb, I in Cs, and F in Rb. The main experimental point established by these figures is that in each case the spectra evolve systematically with changing impurity concentration, c, and clearly define a limiting behavior as $c \to 0$. These are the impurity spectra of principal interest here.

The curves shown in Figs. 2–5 are normalized to display the impurity signal *per impurity atom* (per cm^2 of substrate). In the absence of interactions among impurities, all curves for a given alkali-halogen system would, therefore, be identical. This is far from the case in Figs. 2–5.

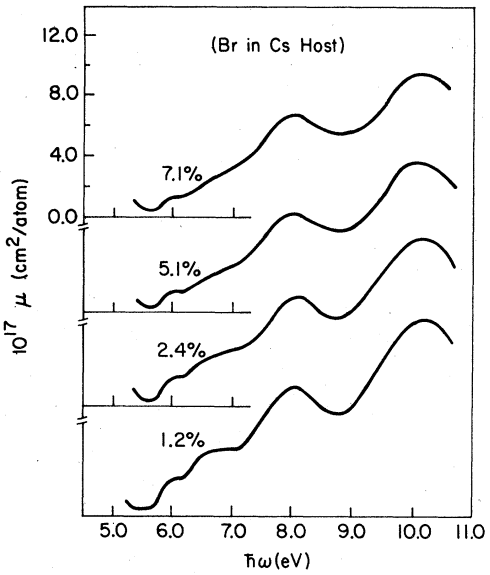

FIG. 2. Absorption spectra per impurity of Br in Cs for Br concentrations ranging from 1.2 to 7.1 at.% (at He temperature).

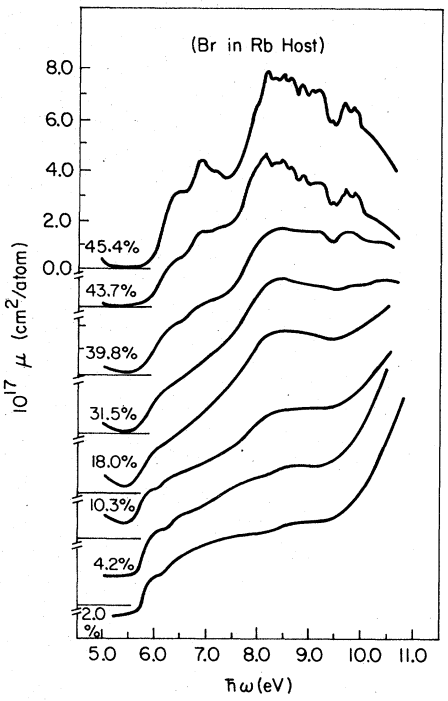

FIG. 3. Absorption spectra per impurity of Br in Rb for Br concentrations ranging from 2 to 45.4 at.% (at He temperature).

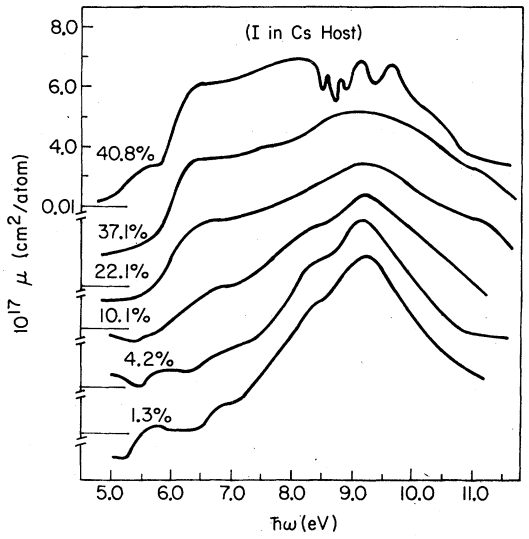

FIG. 4. Absorption spectra per impurity of I in Cs alloys for I concentrations ranging from 1.3 to 40.8 at% (at He temperature).

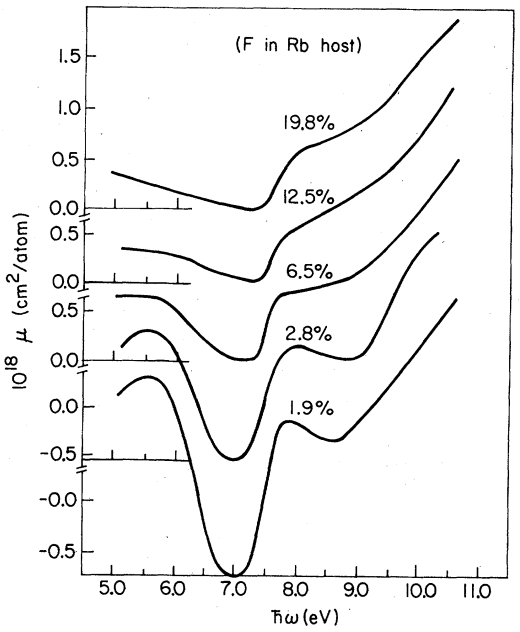

FIG. 5. Absorption spectra per impurity of F in Rb alloys for F concentrations ranging from 1.9 to 19.8 at.% (at He temperature).

Very considerable shifts of oscillator strength distribution with composition are observed in a number of cases. In what follows we are concerned mainly with the results for $c \to 0$, which identify properties of relatively simple materials in which each halogen is isolated in an expanse of host lattice. Before restricting attention to this limit we shall identify some particular features of the impurity interaction effects.

The overall trend of the results can be seen most clearly from the case of Br in Rb (Fig. 3). Sharp peaks begin to emerge at $c = 45$ at.% Br near the metal insulator transition (see Paper I). At this point the spectrum begins to resemble the salt RbBr spectrum quite noticeably. The results for high impurity concentrations were not taken in a particularly critical way, and we caution against their detailed use. Some features of the data are, however, quite well established. In particular, the spin-orbit splitting of the Br core $(4p^6)^-$ configuration is clearly visible in the threshold above 6 eV. With some shifts of oscillator strength, the $4p$ core threshold can now be followed as a function of composition from 45 at.% down to 2 at.% Br. In this dilute limit the threshold is shifted somewhat below 6 eV, but the same spin-orbit splitting is evident in the threshold shoulders. Clearly, these must be Br^- excitations at dilution in the metal. The shoulders identify the predicted charge-transfer excitations. A notable feature of the data is that continuum absorption exists below this excitation threshold.

Similar splittings are visible for the Br spectrum in Cs (Fig. 2), and larger splittings characteristic of I^- appear above 5 eV for I in Cs (Fig. 4). The threshold steps (per impurity) are reduced markedly with increasing impurity content in the Cs data (Figs. 2 and 4), so that little sign of the charge-transfer threshold remains for $c \gtrsim 10$ at.% halogen. These effects of concentration on oscillator strength are likely to be real, since exactly the opposite trend is seen for Br in Rb. There, the threshold shoulder broadens and shows some reduction, but finally increases in size beyond ~18 at.% Br. This eliminates the possibility that the effects arise from some systematic measurement error.

We note also that the total areas under the different spectra remain rather insensitive to composition over very wide composition ranges. This is to be expected from the f sum rule, provided that spectral shifts are small compared with the scan width. The fact that this sum rule is at least approximately satisfied in the present data adds significantly to the confidence with which both the compositions and the optical spectra may be accepted as correct.

The case of F impurities is clearly different from the remainder. At low compositions, the fluorine impurities cause a spectra dip near 7 eV in Rb, but the dip is rather small in amplitude compared with the spectral features caused by the other impurities (note the scales in Figs. 2–5). The dip changes smoothly into a shoulder as the concentration is increased to ~20%. Fea-

tures of this type are not confined to the Rb host system: various similar effects are observed with F in other alkali hosts.

Before leaving the concentration-dependent effects we comment on the spectra of Cl in K presented in Fig. 6. The upper curve shown there is for a sample with 1.2 at.% Cl introduced into K by coevaporation of KCl. The lower curve show the spectrum for a sample with ~2 at.% Cl introduced into the metal in the form of Cl_2 gas. An absolute calibration error of ~20% appears to exist between the two methods of sample preparation. This could be reduced by a factor of perhaps 5 with added care in gas handling, but the effort was not judged worthwhile in view of the corrosive nature of the halogen gas. The main point is that very similar profiles are obtained in the two cases, so that the use of either preparation procedure would probably be satisfactory in practice.

B. Spectra in the dilute limit

The spectra presented in this section are for very dilute solutions. It may be assumed on the basis of the observed concentration dependence that the halogen impurities in the materials do not interact with each other. In this limit, the excitation conditions are as similar as possible to those required for the predicted charge-transfer excitations. Rather well-defined excitation processes do in fact take place for all halogens in the expected energy range. This is made obvious by Fig. 7, where spectra are displayed for all halogens at dilution in K. Potassium is a particularly favorable host lattice which has greater transparency than Li, Rb, or Cs, and also lacks a complication present for Na (see below).

A number of systematic trends are apparent in Fig. 7. In the first place the thresholds for

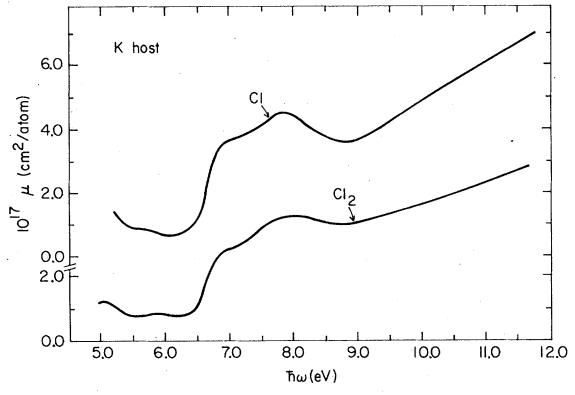

FIG. 6. Absorption spectra of dilute Cl in K for (a). Cl deposited by KCl evaporation and (b) Cl deposited as diatomic Cl_2 gas.

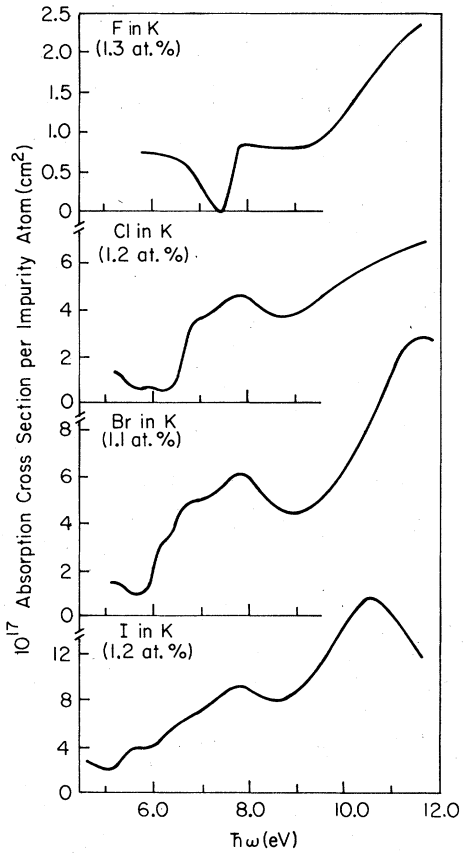

FIG. 7. Absorption coefficient per halogen impurity for F, Cl, Br, and I in potassium (at helium temperature).

the charge-transfer excitation increase steadily from about 5.4 eV for I to well over 7 eV for F. Second, the heavy halogens, I and Br, exhibit spin-orbit splittings at threshold that are identical with those observed in salts. A third point is that the threshold edges of the halogens are not very sharp. They extend over much the same energy range in all cases, as if each is convolved with a common broadening function. This broadening is sufficient to conceal any saltlike spin-orbit splitting for Cl and F.

A fourth noteworthy feature of the data is that the absolute height of the two threshold components sums to approximately 4×10^{-17} cm^2/atom for each of the impurities I, Br, and Cl, but is much smaller for F. Indeed, the F threshold appears more as a dip in a continuum of absorption which is visible below threshold for each of the four impurities. A careful examination of Fig. 7 reveals that dips of similar magnitudes occur below threshold for each of the heavier halogens also. The dips appear less striking for cases other than F because they are much smaller

in magnitude than the threshold step. With respect to the continuum it is notable that the magnitude decreases systematically from about 2×10^{-17} cm^2/atom to 0.7×10^{-17} cm^2/atom in passing from I to F. A final point is that marked peaks occur at about 8 eV in the spectra other than for F, and that large masses of oscillator strength are apparent at still higher energies in all four cases.

It is also of considerable interest to compare spectra of a particular impurity for several different hosts lattices. Figure 8 shows data for Br in Cs, Rb, K, and Na. The case of the Li host is not adequately accessible because of strong host absorption in the energy range near 6 eV. The data in Fig. 8 show strikingly erratic trends of absorption profile with host species. The one feature that reproduces systematically is the spin-orbit split threshold shoulder for Br in Cs, Rb, and K. Even this is eliminated for Na by a curious interference effect and the high plasma energy (5.9 eV) which make the impurity data apparently useless. A second feature that exhibits important systematic changes from one host to the next is the height of the threshold steps. They vary from about 4.3×10^{-17} cm^2/atom for K through 3.2×10^{-17} cm^2/atom for Rb to $\sim3.0\times10^{-17}$ cm^2/atom for Cs. Apart from these two trends, the profiles in Fig. 8 exhibit no detectably systematic change with host species. Even the threshold processes appear rather different in shape

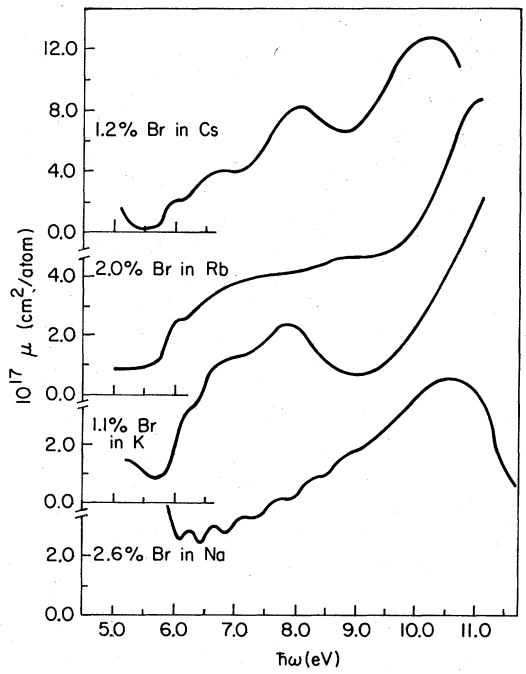

FIG. 8. Absorption coefficient per Br impurity in Na, K, Rb, and Cs host lattices (at He temperature).

for Rb than for K and Cs, as also do the peaks of oscillator strength near 8 and 11 eV. These latter features do not appear to reproduce reliably with either the host or solute species and must therefore be derived in part from properties of each. It should be mentioned that each of the curves presented above have been substantiated by studies of concentration dependence similar to those in Figs. 2–5, or by multiple repetition involving several different dilute alloys.

The oscillatory effects caused by impurities in Na have been reported previously. An example is provided in Fig. 9 by the case of F at 1.9 at.% concentration in a 2700-Å-thick Na film. It appears that these may be ordinary thin-film interference effects modified by the unusual dielectric properties of the plasma and the impurities.[15]

Fluorine behaves so differently from the other halogens that its properties were judged to be worth further investigation. The F spectra observed for the dilute limit in Cs, Rb, K, Na, and Li are presented in Fig. 10. Once more, the variations of absorption profile with host lattice are imperfectly systematic. A common feature for Cs, Rb, K, and Li is the strongly rising absorption at the high-energy end of the figure. A second, to which Na also conforms, is the dip apparent near 7 eV in Cs, which shifts systematically to 9 eV through the sequence Cs-Li. This feature is presumably the charge-transfer excitation. The dip appears to have a progressively broader high-energy edge as the host cell size is reduced (i.e., in the series Cs-Li). No other systematic trends of shape or amplitude are clearly apparent in the data of Fig. 10.

IV. DISCUSSION

A number of interesting phenomena revealed by the data deserve further comment. It will be

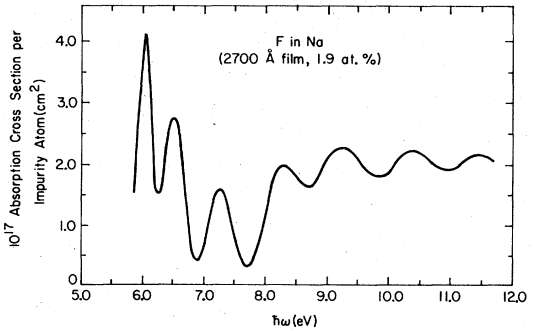

FIG. 9. Absorption cross section per impurity for 1.9 at.% F in Na with a film $\sim$2700 Å thick (at He temperature).

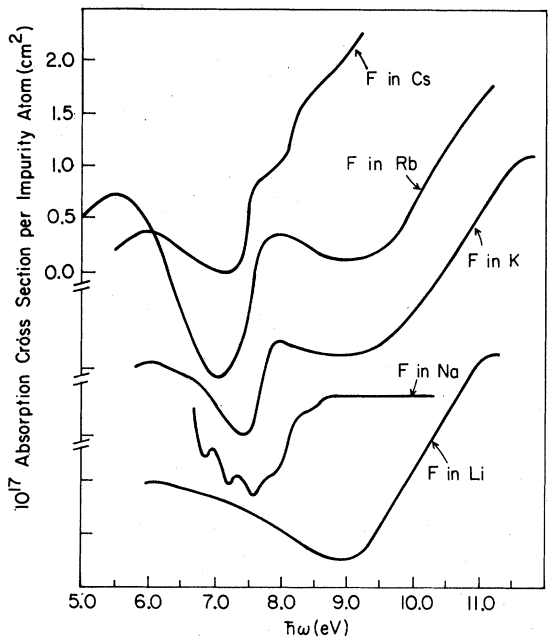

FIG. 10. Absorption cross section per F impurity at dilution in alkali-metal hosts.

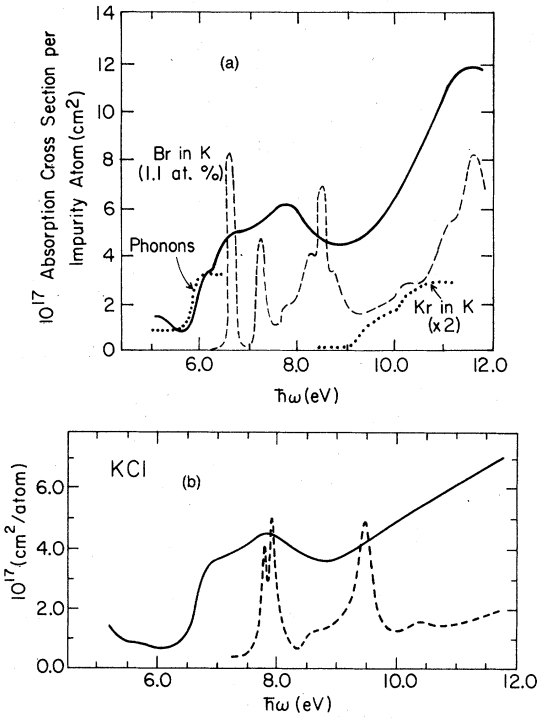

FIG. 11. (a) Absorption coefficient per Br impurity in K compared with the absorption (arbitrary units) of KBr thin films (Ref. 22) (dashed line) and with the absolute absorption profile for dilute Kr in K hosts (Ref. 13). The dotted line near 6 eV shows a Gaussian edge having the theoretical width for phonon effects. (b) Absorption coefficient per Cl in K host compared with that of the KCl salt (Ref. 22), as in (a).

assumed in this discussion that the spectra presented in Sec. III do arise from local excitations of the halogen $(p^6)^-$ ground state. If the theoretical evidence for this assignment were not sufficient, the spin-orbit splittings observed in the Br and I spectra would establish this beyond doubt. The residual resistivities reported in Paper I lend further convincing evidence that the ground state is the negative halogen ion. The halogen resistence is a factor ~3 larger than the rare-gas resistance, and this is consistent with the doubled size of the screening hole in the electron gas. Finally, the identification of the halogen ground state as ionic is placed beyond doubt by the considerable similarity observed in some cases between the impurity spectra and the excitation spectra of the analogous salts. This latter point is illustrated by the comparison in Fig. 11 of the spectra for Cl and Br in K with reported spectra for the KCl and KBr salts.[22] It is clear from Fig. 11 that the metal spectra are blurred and red shifted from the salt spectra, but that all the major splittings and masses of oscillator strength reproduce from the metal to the salt. This similarity finds its explanation in the identical chemical characteristics of the charge-transfer excitation in metals and the exciton process in salts.

A. Charge-transfer excitations

The purpose of this section is to summarize and interpret the evidence concerning the energies of the lowest locally excited configurations of the halogens in alkali host lattices. The substantial absorption continua observed below the threshold for these charge-transfer excitations will be discussed in Sec. IV C and are not of interest here. Optical charge-transfer thresholds are identified as the lower of the spin-orbit split features apparent for I and Br impurities, and the analogous unsplit features in the spectra of Cl and F. For reasons explained below, it is the half-height of the threshold step that is identified as the actual optical energy of interest here.

Table I is a compilation of threshold properties, with the observed energies $\hbar\omega_{exp}$ gathered in column 4. Column 2 gives the thermal charge-transfer energies $\hbar\omega_t$ predicted by Flynn.[3] These should differ from the observed optical energies by a Stokes' shift associated with lattice strains in the excited state reached suddenly by the optical transition. Values given in parentheses are obtained by smooth interpolation among the two-dimensional network of values for which pre-

TABLE I. Thermal charge-transfer energies $\hbar\omega_t$ (as predicted by Flynn, Ref. 3) differ by a relaxation energy E_r from the observed threshold energies $\hbar\omega_{exp}$. The theoretical energies $\hbar\omega_{th}$ obtained using Eq. (6) are in good agreement with the observed values.

	$\hbar\omega_t$	E_r	$\hbar\omega_{exp}$	$\hbar\omega_{th}$
LiF	(~6)	~4	10.0	~(9.2)
NaF	5.98	2.02	8.0	7.96
NaCl	5.17	•••	•••	7.15
NaBr	4.35	•••	•••	6.33
NaI	3.40	•••	•••	5.38
KF	6.26	1.42	7.68	7.69
KCl	5.17	1.47	6.64	6.60
KBr	(4.5)	(1.5)	6.03	(5.9)
KI	(3.8)	(1.5)	5.33	(5.2)
RbF	(6.4)	(1.1_5)	7.55	(7.4)
RbCl	(5.2)	•••	•••	(6.2)
RbBr	(4.7)	(1.1_5)	5.85	(5.7)
RbI	(4.1)	•••	•••	(5.1)
CsF	6.53	0.97	7.50	7.64
CsCl	5.30	•••	•••	6.41
CsBr	(4.9)	(0.9)	5.82	(6.0)
CsI	4.49	0.97	5.46	5.60

dictions are available. For example, the value of 6.4 eV for RbF is obtained from the values 6.53, 6.26, and 5.98 eV for CsF, KF, and NaF, and the value of 3.8 eV for KI from the available values for NaI (3.40 eV) and CsI (4.49 eV). No direct predictions are available for bromides, but the threshold energy for KBr can be estimated with confidence from values in the sequence KF, KCl, and KI, and CsBr from CsF and CsI, together with other typical sequences such as KF-KI. The network of predicted values obtained in this way is probably correct to ~0.2 eV.

These results make an interesting comparison with the observed optical thresholds in column 4. The observed energies are uniformly larger than the predicted value, as expected for a Stokes' shift. Most important is the fact that the observed shifts, collected in column 3, are almost identical for all ions in a given solvent, and that the values for different solvents behave in a systematic way. They are as follows: Li: 4 eV; Na: 2.0 eV; K: 1.5 eV; Rb: 1.15 eV; Cs: 0.95 eV.

To interpret these results we recognize that the energy of the local center depends significantly on lattice relaxation. The Coulomb energy of the impurity ion coupling to the surrounding unscreened ions must be proportional to the fractional local expansion ϵ of the defect cell. Moreover, the strain energy in the lattice must be proportional to ϵ^2. We thus write the total energy change with ϵ as

$$E(\epsilon) = \alpha\epsilon + \beta\epsilon^2 . \tag{1}$$

The energy change from $\epsilon = 0$, to its minimum value at

$$\epsilon_0 = -\alpha/2\beta \tag{2}$$

is

$$E_r = -\alpha^2/4\beta . \tag{3}$$

It is shown in the Appendix that simple models yield the result that

$$\alpha \propto e^2/r_s ; \quad \beta \propto r_s^3/\chi , \tag{4}$$

with r_s the cell radius and χ the compressibility. Thus

$$E_r = A\chi/\Omega^{5/3} , \tag{5}$$

with Ω the atomic volume and A a single constant for all impurities and host lattices. Accordingly, the predicted excitation energies are

$$h\omega_{th} = h\omega_t + A\chi/\Omega^{5/3} . \tag{6}$$

The values of $\hbar\omega_{th}$ shown in column 5 of Table I are obtained from Eq. (6) with the value of A chosen as 2.7×10^7 (eV), when χ is expressed in kg/cm^2 and Ω is the molar volume in cm^3.[16] They are in very good agreement with the experimental results. In no case does the observed deviation exceed 0.15 eV for the five cases NaF, KF, KCl, CsF, and CsI for which experimental and theoretical values are both available. For the additional five cases of KBr, KI, RbF, RbBr, and CsBr, for which interpolated values of $\hbar\omega_{th}$ are given in Table I, the predictions are in equally good agreement with the observations. The extrapolated case of LiF is somewhat less successful, with an observed broad threshold near 10 eV to be compared with the predicted value of 9.2 eV.

A final point in connection with this model is that the constant $A = 2.7\times 10^7$ (eV) is reproduced rather well by an approximate theoretical analysis of the strain problem. It is shown in the Appendix that

$$A = (\epsilon_0 a_0)^2 (2\pi)^{2/3} N_A^{5/3} (1+\sigma)/24(1-2\sigma) . \tag{7}$$

In Eq. (7) ϵ_0 is the Hartree, a_0 is the hydrogen radius, N_A is Avogadro's number, and σ is Poisson's ratio for the host lattice, typically 0.34 for alkali metals. This result gives

$$A = 2.23\times 10^7 \text{ (eV)} . \tag{8}$$

The agreement of the approximate theoretical value with the empirical value required in Eq. (6) is as good as could be expected. It confirms beyond reasonable doubt the origin of the observed threshold shifts in lattice strain effects.

A second feature of the data bears on the ques-

tion of lattice contributions to the optical threshold. It is well known that, in the linear coupling approximation, the same electron-lattice interactions that Stokes' shifts the transitions also cause a broadening of the spectrum.[17] In effect, the underlying transition profile is convolved with a Gaussian phonon broadening function of rms width (at 0 °K) given by

$$W \simeq 2\sqrt{E_r E_0}\ . \tag{9}$$

Here, E_0 is the zero-point phonon energy per atom and $E_r = \hbar\omega_{\rm exp} - E_t$ is the Stokes' shift.

Equation (4) offers an immediate explanation for the observation (see Sec. III) that all the halogen impurities in K exhibit almost identical threshold broadenings. This is now explained by the fact that all halogens have the same Stokes shift E_r in a given host, and that the same zero-point energy (that of K) is relevant in each case. Some guess as to the form of the underlying threshold is needed in order to derive an actual predicted threshold profile for comparison with experiment. The dotted line in Fig. 11 shows the profile obtained by convolving a square step edge with a Gaussian of width W given by expression (9) with $E_r = 1.5$ eV and $E_0 = 4$ meV. It is indistinguishable from the experimental profile, thereby lending substantial confirmation to our identification of the threshold shifts with lattice processes.

A final point is that the broadenings of the edges observed in Cs and Rb are smaller by a factor ~1.6 than that for K. This is quite adequately consistent with Eq. (9) together with the known Debye temperature difference[16] (a factor ~2) and the observed Stokes' shift difference (a factor ~1.4). These data will warrant a fully quantitative analysis when the theory of the underlying line profile is better developed.

To summarize this section we note that the observed optical thresholds $\hbar\omega_{\rm exp}$ deviate from the predicted thermal energies by the expected positive energy difference. This energy difference takes values sensibly independent of the particular halogen, but differing among the various alkali host lattices. The optical thresholds of ten systems can be predicted within ~0.2 eV by a simple identification of the shifts as lattice energies associated with Coulomb fields in compressible lattices. Further confirmation of this analysis of the threshold energies is supplied by the threshold roundings, which are accurately reproduced by a Gaussian convolution of width given by Eq. (4), for an assumed underlying step function edge. The common broadenings observed for all halogens in a single host, and the changes of threshold rounding that are observed from one host to the next, are all directly predictable from the present model presented here.

One therefore concludes that the present observations do indeed identify the charge-transfer process. The energetics of the charge transfer are evidently rather well understood, and conform quite accurately to prior theoretical predictions. In what follows, the discussion center on other areas that are much less well understood.

B. Shape of the persistent optical profile

This section gathers together the facts concerning other features and the data presented in Sec. III. Only the position, the Gaussian shape, and the spin-orbit splitting of the threshold process have been discussed in previous sections of the paper. Below threshold there exist both continuum absorption and a marked threshold dip that are each of some interest. Above threshold there is much detailed information about higher persistent states. The behavior below threshold constitutes a rather separate topic that is deferred to Sec. IV C. The discussion that follows concerns the observed optical absorption for $\hbar\omega > \hbar\omega_{\rm exp}$.

Perhaps the most striking feature of the oscillator strength distribution in charge-transfer excitations is its similarity to that of the analogous salts (see Fig. 11). The general occurrence of these parallel trends in dissimilar hosts is easily explained. Excitations in salts remove an electron from the full halogen $(p^6)^-$ shell (valence band) and transfer it to a conduction band which is largely derived from cations orbitals. But this is exactly what happens in the metal, also, when a halogen impurity core contributes an electron *to its neighboring alkali atoms* (see Fig. 1) as a result of the charge-transfer process. Clearly, the common features of the two spectra must arise from close chemical similarities between the two excitation processes.

In this latter connection it seems worth remarking that the present data have some relevance to the analysis of excitons in salts. Since the host lattices are very different for excitons and charge-transfer excitations (one is a metal and the other a salt), it seems fair to say that similarities can arise only from processes that are strongly localized at the halogen and its immediate alkali neighbors. To the extent that the coarse distribution of oscillator strength with energy is recognizably similar in the two cases, it appears that the two spectra must be dominated by local properties. While band arguments applied to the salts can be used to eventually reproduce the relevant local effects, this route to the prediction

of essentially local properties may be unnecessarily circuitous. A "local orbital" approach appears more efficient.

Some charge-transfer spectra are sufficiently similar to the salt spectra (e.g., Fig. 11) to tempt numerical analysis. This is also the case in the comparison of spectra for rare-gas impurities in metals with the analogous spectra for solid rare gases.[13] Figure 11 shows that the principal features of the salt spectra are red shifted and broadened to produce the impurity excitation profile in the metal, but are otherwise largely unchanged. The question arises as to whether or not a convolution of the salt (or rare-gas) spectrum with some broadening function characteristic of the host metal could possibly produce an acceptable halogen (or rare-gas) impurity spectrum. A response function of this type, characteristic of the metal, would clearly be of fundamental interest.

Unfortunately, it appears that no simple convolution interrelates the two spectra. In the KBr spectrum of Fig. 11, for example, the lower-energy spin-orbit partner must continue under the higher-energy component in order to reproduce the height of the second component by duplicating the first with an appropriate scaling and shift. However, the tail thereby created on the convolving function makes it impossible to reproduce the third peak at 7.7 eV from the (triplet) peak near 8.7 eV in the salt spectrum. One is drawn to the conclusion that (to the extent these procedures make any sense) the p^5d and p^5s structures undergo different shifts between the salt and metal lattices; the convolution approach therefore breaks down. Given the complications of the underlying continuum and the threshold dip (see Sec. IV C) the phonon broadening, the presence of different shifts, and possible changes in relative p^5s and p^5d oscillator strength, any attempt at a quantitative decomposition of the impurity spectrum now degenerates into guesswork. The similarities between the spectra are readily apparent to the eye, but the quantitative relationship is obscure.

Semiquantitative comments can be made in one area, but the conclusions nevertheless leave the major puzzles unresolved. This is in the area of the threshold behavior. It seems reasonably safe to conclude (Sec. IV A) that the shape of the charge-transfer threshold is largely phonon determined. The lack of excess threshold broadening then implies that the electronic excitation spectrum underlying the phonon convolution is a sharp step edge, at least on the scale of 0.2 eV relevant, for example, to the well-documented threshold edges of Br in Cs (Fig. 2). The similarities among the threshold processes for all the halogens makes it plausible that the electronic spectrum is a step of width $\lesssim 0.1$ eV. Some spectra (e.g., I in Cs, Fig. 4) appear to suggest that the step might possess extra strength near the threshold energy itself. A behavior of this type is by no means incompatible with theories that predict threshold profiles in terms of phase shifts undergone by Fermi-surface electron scattering of the ground and excited states.[8,9] From infinite barrier phase shifts (see Paper I), for example, one predicts a weak divergence,[8]

$$f(E) \sim [\hbar(\omega - \omega_{\mathrm{exp}})]^{-0.18},$$

at threshold, which may possibly be consistent with the appearance of the Gaussian broadened threshold profiles displayed in Sec. III.

The real puzzle arises from the variation of threshold profile from one element to the next. The halogens, the rare gases, and the alkali metals are successive elements in the Periodic Table. The threshold behavior of each of these species in alkali hosts has now been established. Figure 12 shows the typical profiles for $p^6 \rightarrow p^5s$ excitations of halogens (as deduced in the present work), rare-gas atoms,[13] and alkali host atoms in the heavy alkali metals.[18] These profiles are shown adjacent to sketches that indicate the electron-density distributions characteristic of the initial and final configuration of the transition.

The alkali and halogen spectra depicted in Fig. 12 are to some extent in acceptable agreement with theory. Almost all realistic values of phase shift changes accompanying local $p^6 \rightarrow p^5s$ excitations produce theoretical threshold behavior that diverges at $\hbar\omega_{\mathrm{exp}}$. The halogen and alkali data can be accommodated within this framework. However, no way has been found to reconcile the excitation profiles of rare-gas atoms in alkali metals with the theory. Moreover, the composite data reveal more than the individual parts. Each of three chemical types produces its own distinctive threshold behavior for $p^6 \rightarrow p^5s$ excitations. These are indicated in Fig. 12. The sequence of thresholds from halogens through rare gases to alkali metals is erratic, and at present lacks any plausible explanation. We can nevertheless deduce that the profiles are a *chemical* property of the excited species. In all three cases it is found that chemically similar elements yield observably similar spectra. The relationship between chemical structure and these excitation profiles remains poorly understood.

A second aspect to this problem is revealed by a comparison of absorption strength above threshold for halogens and rare gases. As mentioned above, the present experimental methods

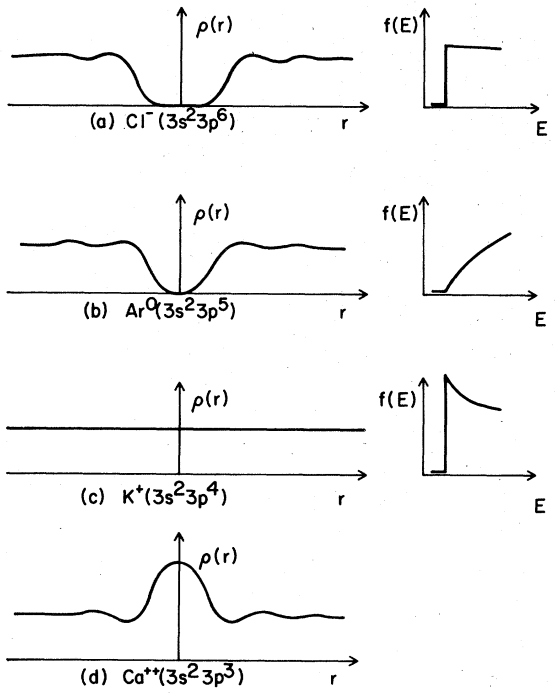

FIG. 12. Conduction-electron density distribution $\rho(r)$ is sketched for (a) the p^6 Cl^- core, (b) the p^6 Ar^0 core, (c) the p^6 K^+ core, and (d) the p^6Ca^{2+} core. One electron is transferred from the Cl^- core to the cell perimeter in the $p^6 \rightarrow p^5s$ charge-transfer excitation, which resembles the transition from (a) to (b). Also sketched are the observed absorption profiles corresponding to the ground-state configurations.

yield *absolute* absorption measurements that allow results from dissimilar impurities to be compared. Figure 11 shows that the absorption amplitude for Kr near threshold is only half that for Br, and a similar comparison holds for Xe with I. The f sum rule imposes a requirement that the p^6 excitations contain a fixed area under the absorption profile. The electronic response to rare-gas excitations must therefore spread the oscillator strength over approximately twice the energy range of that for halogens. No explanation of this fact is available at present.

Since one-particle matrix elements are probably larger for rare gases than for halogens, it seems likely that the observed threshold amplitudes must be strongly influenced by many-particle phenomena. This point concerns the optical matrix elements $\langle\phi|\nabla|\psi\rangle$ that connect core orbitals ϕ of the initial state to band orbitals ψ of the final state. The excited s orbital of the rare gas overlaps fully with the initial core (see Fig. 12), whereas that for the halogen does not. For these reasons the one-particle optical matrix elements are probably larger for rare gases than for halogens. The observed opposite trend must be attributed to other causes.

One feature of the threshold amplitudes that appears in part comprehensible is its trend with halogen species in a given host lattice. The fact that F is much smaller than the other halogens must reduce its overlap with electrons outside the excited-state screening hole below the values for the other halogens. This indication that the optical matrix elements may be small is certainly consistent with the small threshold amplitude observed for F. Some evidence for similar amplitude trends with host and impurity cell size is discernable in Figs. 10, 2, and 3, although the threshold amplitudes for F in different alkali metals are seen in Fig. 10 to vary in an apparently erratic way.

We conclude this section by noting that few aspects of the optical excitation profile are understood even semiquantitatively. The discernable persistence of spectral features between salts and metals points to the dominance of local properties in both. The erratic variation of profile among metal hosts also points to the part played by metal atoms in determining the spectrum. Apart from these qualitative points, very little is understood. No simple, quantitative relationship exists between the spectra characteristic of a particular atom in different environments. Neither the amplitudes of the threshold profiles, nor their variation from one chemical species to the next can be explained by available theories.

C. Continuum absorption and interference

This section contains brief comments about the continuum absorption observed below threshold. Evidently the addition of halogen and alkali atoms by alkali-halide evaporations causes extra absorption in the experimental energy range. We note that the continuum absorption per added alkali atom $\sim 10^{-17}$ cm^2/atom is comparable with the alkali absorption coefficient per atom in the pure metal.[19] The effect is also consistent in order of magnitude with the extra scattering of conduction electrons caused by the halogen impurities. Using Drude theory one obtains the result

$$\mu_i \simeq \mu_0 \rho_i / \rho_0$$

in which the change μ_i/μ_0 of absorption is related to the change ρ_i/ρ_0 of resistance introduced by the impurities. This formula predicts, for example, a residual resistivity for Br in Rb of ~ 10 $\mu\Omega$ cm/at.% as compared with an observed value of 6 $\mu\Omega$ cm/at.%.

Drude theory is, of course, wholly unreliable in the energy range above the plasma frequency.

Moreover, the preceeding comparison of extra alkali absorption with host absorption is also complicated by the fact that the extra alkali atom enters the alloy as an *ion* lacking a valence electron. Neither of these explanations of the continuum absorption is therefore quantitatively acceptable. Nevertheless, the effects they simulate do undoubtedly exist, and it seems likely that the observed absorption originates in a combination of these two causes.

The absorption dips observed immediately below threshold appear to be caused by Fano interference processes. Beautiful examples of these effects are observed in atomic spectroscopy when a sharp local configuration is connected to a continuum process by an intrinsic decay mode.[20] Similar effects have also been observed for deep core levels in solids.[21]

In the present case the coupling evidently exists between the charge-transfer process and the background excitation continuum arising from the perturbed electron gas. We note that the charge-transfer process is longitudinal in character, and it undoubtedly couples strongly to plasmonlike electron gas excitations. At the same time, an excited halogen may well decay by recombination with a conduction electron and the simultaneous excitation of an electron-hole pair in an Auger-like process. The existence of a coupling between the local process and the band continuum therefore appears reasonable, regardless of the imperfectly defined nature of the band excitations. Unfortunately, the phonon broadening of the interference profile (Sec. III A) precludes the possibility of obtaining the coupling strength from the observed profile.

Interference effects from local excitations in a metal may possess considerable theoretical implications. If the underlying continuum consists mainly of single electron-hole pair creation processes, then the coupling of the charge-transfer excitation process to these final states presumably implies that it, too, involves few quasiparticle pairs. This is in contradiction with MND theory, which predicts that a divergent density of electron-hole pairs is created by local excitations near threshold.[8,9] An indication that few pairs are, in fact, created has previously been deduced from studies of rare-gas spectra in alkali-metal host lattices.[13] Support for this deduction has also been provided by the calculations of Kittler and Falicov,[4] and Dow and Flynn.[12]

V. CONCLUSIONS

The principal result of this work is to confirm the existence of charge-transfer excitations as long-lived locally excited configurations of halogens in alkali metals. The excitation thresholds are accurately predicted when allowance is made for the coupling of the optical transition to the lattice. All spectral features are broadened to an extent compatible with this coupling. The spectra resemble those of salts in a discernable but non quantitative way indicating that both excitons and charge-transfer processes probe local properties. Quantitative interpretations of most spectral features are still lacking. In particular, the threshold profiles for local excitations in metals remain poorly understood.

ACKNOWLEDGMENT

Support for this research by the NSF under the MRL Grant No. DMR-77-23999 is gratefully acknowledged.

APPENDIX

In this Appendix we present an approximate calculation of the Stokes' shift exhibited by the halogen excitations. It is simplest to consider the emission process, relying on the fact that in the present linear coupling approximation, the absorption and emission Stokes' shifts are of equal magnitude.

The excited halogen consists of a neutral atom in a solvent cell. Both the cell and surrounding lattice are neutral because conduction electrons are largely excluded from the impurity cell. In the ground state, the halogen ion repels electrons more and, in a jellium model, a shell of positive charge is located around the impurity. Simplified electron and background lattice charge distribution are shown in Fig. 13.

When the impurity ion couples to this positive shell, the energy of the lattice can be lowered by an inward relaxation. The coupling energy is

$$E_c = -e^2/r_1(1+\epsilon)\,, \tag{A1}$$

with r_1 the shell radius and ϵ the fractional relaxation. This is resisted by the lattice strain energy[23]

$$E_s = 8\pi\mu r_2^3\epsilon^2\,, \tag{A2}$$

with μ the shear modulus and r_2 the radius at which the lattice strain starts. The shear modulus is obtained from the compressibility χ as

$$\mu = 3(1-2\sigma)/2(1+\sigma)\chi\,, \tag{A3}$$

with σ Poisson's ratio. One thus finds the total energy

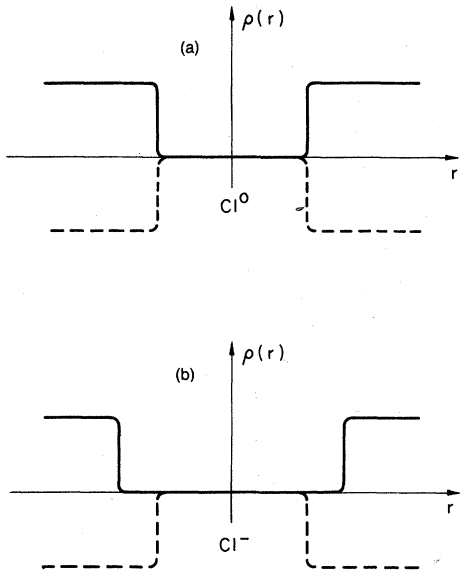

FIG. 13. Sketch showing the (negative) charge density in the lattice near the Cl^- ground state (b) and the Cl^0 excited state (a) including electron density (solid lines) and positive background charge (broken lines). The screening of the Cl^- state by repelled electrons exposes a shell of positive charge, thereby causing Stokes' shifts (see text).

$$E = -\frac{e^2}{r_1(1+\epsilon)} + \frac{12\pi(1-2\sigma)r_2^3\epsilon^2}{(1+\sigma)\chi}; \tag{A4}$$

the relaxation energy

$$E_r = -\left(\frac{e^2}{r_1}\right)^2 \frac{(1+\sigma)\chi}{48\pi(1-2\sigma)r_2^3} \tag{A5}$$

then follows as explained in Sec. IV A. One can therefore write the Stokes' shift in the form

$$E_r = -A\chi/\Omega^{5/3}, \tag{A6}$$

with

$$A = \left(\frac{e^2}{a_0}\right)\frac{(1+\sigma)a_0^2}{36(1-2\sigma)}\left(\frac{4\pi}{3}\right)^{2/3}\gamma_1\gamma_2 \tag{A7}$$

and

$$\gamma_1 = 4\pi r_1^3/3\Omega^3; \quad \gamma_2 = 4\pi r_2^3/3\Omega. \tag{A8}$$

γ_1 and γ_2 then define the radius at which the positive charge density exists and the lattice strain starts, respectively.

Neither the charge density nor the "lattice strain" are particularly well defined in the real impurity-host complex. The value $\gamma = 1.5$ identifies the middle of the region of electron deficiency (i.e., the region between spheres of radii Ω and 2Ω) and we shall adopt the estimate

$$\gamma_1 = \gamma_2 = 1.5. \tag{A9}$$

One thus finds

$$A = \left(\frac{e^2}{a_0}\right)\frac{a_0^2}{24}\frac{(1+\sigma)}{(1-2\sigma)}(2\pi)^{2/3}N_A^{5/3}. \tag{A10}$$

For the choice $\sigma = 0.34$ typical of alkali metals,[16] this result gives $A = 2.231\times10^7$ (eV), with χ measured in kg/cm^2 and Ω in cm^2/mole. The predicted Stokes shifts for all halogens in the different alkali metals are then: Li: 2.6 eV (~4 eV); Na: 1.6 eV (2.0 eV); K: 1.2 eV (1.5 eV); Rb: 0.85 eV (1.15 eV); Cs: 0.92 eV (0.95 eV) in which the experimental values are indicated in parentheses for comparison. The theoretical predictions are, of course, in as good agreement with the data as could be expected from the present simplified methods. A second comparison is provided by the experimentally deduced value $A = 2.7\times10^7$ (eV), which lies within 20% of the value $A = 2.23\times10^7$ (eV) calculated in this Appendix.

[1]R. Avci and C. P. Flynn, Phys. Rev. B 19, 5967 (1979) (preceding paper).
[2]C. P. Flynn and N. O. Lipari, Phys. Rev. Lett. 27, 1365 (1971).
[3]C. P. Flynn, Phys. Rev. B 9, 1984 (1974).
[4]R. C. Kittler and L. M. Falicov, Solid State Commun. 20, 973 (1976).
[5]C. P. Flynn and N. O. Lipari, Phys. Rev. B 7, 2215 (1973); C. P. Flynn, Phys. Rev. 14, 5294 (1976).
[6]C.-O. Almbladh and U. von Barth, Phys. Rev. B 13, 3307 (1976).
[7]G. Bryant, Phys. Rev. (to be published).
[8]For a review, see G. D. Mahan, *Solid State Physics* (Academic, New York, 1974), Vol. 29.
[9]P. Nozières and G. T. De Dominicis, Phys. Rev. 178, 1097 (1969).
[10]D. L. Smith and J. D. Dow, Phys. Rev. B 9, 2509 (1974); C. P. Flynn, Phys. Rev. Lett. 37, 1445 (1976); C.-O. Almbladh, Phys. Rev. B 16, 4343 (1977); C.-O. Almbladh and P. Minnhagen, *ibid.* 17, 929 (1978).
[11]R. P. Gupta and A. J. Freeman, Phys. Rev. Lett. 36, 1194 (1976).
[12]J. D. Dow and C. P. Flynn, J. Phys. C (to be published).
[13]D. J. Phelps, R. A. Tilton, and C. P. Flynn, Phys. Rev. B 14, 5254 (1976).
[14]W. H. Lawson, J. Sci. Instrum. 44, 917 (1967).
[15]The authors wish to thank Ms. W. Chen and Professor K. Kliewer for helpful discussions of these effects.
[16]See tabulations by K. Gschneidner, *Solid State Physics* (Academic, New York, 1964), Vol. 16.
[17]See, e.g., T. H. Keil, Phys. Rev. A 140, 601 (1965).
[18]T. Tshii, Y. Sakisaka, and S. Yamaguchi, J. Phys. Soc. Jpn. 42, 876 (1977); R. Haensel, G. Keital,

P. Schreiber, B. Sonntag, and C. Kunz, Phys. Rev. Lett. 23, 528 (1969).
[19]U. S. Whang, E. T. Arakawa, and T. A. Gallcott, Phys. Rev. B 6, 2109 (1972).
[20]H. G. M. Heideman, W. V. Dalfsen, and C. Smith, Physica 51, 215 (1968); U. Fano and J. W. Copper, Rev. Mod. Phys. 40, 441 (1968); U. Fano, Phys. Rev. 124, 1866 (1961).
[21]R. E. Dietz, E. G. McRae, Y. Yafet, and C. W. Caldwell, Phys. Rev. Lett. 33, 1372 (1974); C. Guillot, Y. Ballu, J. Paigne, J. Lecante, K. P. Jain, P. Thiry, R. Pinchoux, Y. Petroff, and L. M. Falicov, *ibid.* 39, 1632 (1977).
[22]See, e.g., K. T. Teegarden and G. Baldini, Phys. Rev. 155, 896 (1967).
[23]For a discussion of these models see, e.g., C. P. Flynn, *Point Defects and Diffusion* (Oxford University, London, 1972).